# Tensor component of the two-nucleon interaction in the quark-bag model

Carleton DeTar

*Department of Physics, University of Utah, Salt Lake City, Utah, 84112*

(Received 21 November 1978)

A previously developed method for computing the interaction energy of the two-nucleon system at short distances in the static MIT bag model of confined quarks is extended to all isospin and spin channels available to the two-nucleon interaction. The present study is restricted to spherical geometries and short distances (separations less than about one F) to simplify the computation. The tensor component of the interaction in the isosinglet and isotriplet channels is found to agree in sign with the accepted phenomenological two-body tensor potential.

## I. INTRODUCTION

In recent months the bag idea for quark and gluon confinement has become increasingly appealing.[1,2] Attempts to explain confinement from first principles in quantum chromodynamics (QCD)[3-7] have suggested that two vacuum phases occur, the stable vacuum having the property that it excludes color-electric flux lines. Hadrons are then regions of ordinary vacuum in which quark and gluon fields may exist, the energy difference per unit volume between the two vacuums being a constant $B$, which can be calculated from the color coupling constant and renormalization scale in QCD. Differences in some details are to be expected between the bag model as derived from QCD and the MIT bag schemes of confinement. However, current indications are promising that the general picture of a hadron in the MIT bag model may well result from a more fundamental theory.

As a phenomenological description of hadronic structure, the MIT bag model must be tested in confrontation with experiment. In this spirit we have studied the two-nucleon interaction at short distances in the static cavity approximation to the bag, using the same parameters and approximations which gave good values for the masses and other static parameters of various light hadrons.[8] We found that in addition to accounting for a repulsive core, the bag model gives a strongly attractive interaction at intermediate range in the channel $I=0$, $S=1$ with spin projection $m_s=1$ along the deformation axis.[9,10] Here we report results of a straightforward extension of the calculation of Ref. 10 to all isospin and spin channels available to the two-nucleon system. Since we are mainly interested in a qualitative result, given our present uncertainty in the precise nature of confinement, we have for the sake of simplicity confined our attention here to hadrons of spherical shapes. It was found in Ref. 10 that the six-quark system assumes a nearly spherical shape for

short distances throughout the repulsive core and out to distances of maximum attraction. In Fig. 1 we reproduce the deformation energy for the channel $I=0$, $S=1$, $m_s=1$ computed for a general three-parameter class of shapes as described in Ref. 10 and compare :          deformation energy for the same channel with only spherical shapes admitted. It is evident that only for $\delta \gtrsim 1$ F does a substantial deviation occur. (For spherical shapes a "deformation" constitutes a shift in the internal quark orbitals and a variation in the radius.) Instead of using the variationally constructed quark orbitals and gluon fields of Ref. 9, which enter into the curve of Fig. 1, we may take the exact solutions for the sphere,[8,9,11] the use of which in any case results in only few-percent differences in the field energies. Another advantage of working with spherical geometries is that the self-energy and zero-point energy may be treated exactly as in Ref. 8, thereby sparing us the necessity of estimating their behavior for nonspherical geometries.[9]

In Sec. II we summarize the principal formulas needed from Ref. 10 and describe the computation. In Sec. III we report and discuss the results. Appendix A summarizes the computation of field energies in the sphere and Appendix B and Table II summarize the internal-symmetry "configuration factors" for the various channels. The combinatoric results of Appendix B are of general interest in calculations in the nonrelativistic quark model as well.

## II. REVIEW OF THE MODEL

We review briefly the key ingredients of the model.[8-10]

### A. The configuration

The spherical cavity of radius $R$ contains six massless quarks, three of which are placed in a "left" orbital and three in a "right" orbital. These
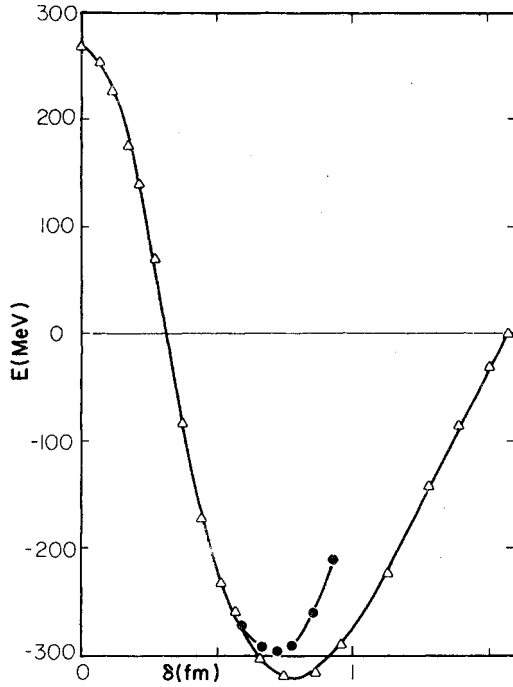
FIG. 1. Comparison of deformation energies for the two-nucleon configuration with $I=0$, $S=1$, $m_s=1$ with the three-parameter cavity shape of Ref. 10 (triangles) and strictly spherical cavities (dots).

orbitals are hybrids of the lowest-energy even- and odd-parity free-fermion cavity eigenmodes. The Dirac spinors for these orbitals

$$q_{Lm}=q_{Sm}-\sqrt{\mu}q_{Pm},$$

$$q_{Rm}=q_{Sm}+\sqrt{\mu}q_{Pm} \tag{2.1}$$

are defined in terms of the $S_{1/2}$ and $P_{3/2}$ eigenmodes[1]:

$$q_{Sm}=\frac{N_S}{\sqrt{4\pi}}\begin{pmatrix} j_0(\omega_S r/R)\mathfrak{U}_m \\ i\vec{\sigma}\cdot\hat{r}j_1(\omega_S r/R)\mathfrak{U}_m \end{pmatrix}e^{-i\omega_S t/R},$$

$$q_{Pm}=\frac{N_P}{\sqrt{4\pi}}\begin{pmatrix} j_1(\omega_P r/R)\mathfrak{U}_{Pm} \\ i\vec{\sigma}\cdot\hat{r}j_2(\omega_P r/R)\mathfrak{U}_{Pm} \end{pmatrix}e^{-i\omega_P t/R}, \tag{2.2}$$

where

$$\mathfrak{U}_{Pm}=\frac{3}{\sqrt{2}}(z-\tfrac{1}{3}\vec{\sigma}\cdot\vec{r}\sigma^3)/R\mathfrak{U}_m \tag{2.3}$$

and $\mathfrak{U}_{1/2}=\binom{1}{0}$, $\mathfrak{U}_{-1/2}=\binom{0}{1}$. The $\mathfrak{U}_{Pm}$ are the $m=\pm\frac{1}{2}$, $j=\frac{3}{2}$ odd-parity spinor harmonics. The axis of separation is the $z$ axis. As the parameter $\mu$ ranges from 0 to 1 the left and right orbitals range from a complete overlap to complete orthogonality. The characterization of left and right can be seen explicitly by computing the baryon-number density

$q_L^\dagger q_L$ which shows a leftward shift as $\mu$ increases.[10] The eigenfrequencies $\omega_S$ and $\omega_P$ are chosen so that when $r=R$ the linear bag boundary condition

$$i\vec{\alpha}\cdot\hat{r}q_n=-\beta q_n \tag{2.4}$$

is satisfied, where $\vec{\alpha}$ and $\beta$ are the Dirac matrices. Thus

$$\omega_S=2.043, \quad \omega_P=3.204. \tag{2.5}$$

The normalization factors are defined so that $\int q^\dagger q\,dV=1$ for each orbital.

Corresponding to each orbital there is a cavity fermion creation operator for the quark

$$b_{Rcfm}^\dagger=b_{Scfm}^\dagger+\sqrt{\mu}b_{Pcfm}^\dagger,$$

$$b_{Lcfm}^\dagger=b_{Scfm}^\dagger-\sqrt{\mu}b_{Pcfm}^\dagger, \tag{2.6}$$

where $c$ and $f$ refer to color and flavor indices. An appropriate linear combination of products of three creation operators $b_R^\dagger$ forms a creation operator for a proton or neutron of the desired spin component in the right orbital—likewise for the left orbital. To form a state with quantum numbers of the deuteron with spin projection $m_s=0$ on the $z$ axis, for example, the nucleon creation operators thus defined are then combined as they should be (in an obvious notation) as follows:

$$N(\mu)|I=0, S=1, m_s=0\rangle$$

$$=[p_R^\dagger(\uparrow)n_L^\dagger(\downarrow)+p_R^\dagger(\downarrow)n_L^\dagger(\uparrow)$$

$$+p_L^\dagger(\uparrow)n_R^\dagger(\downarrow)+p_L^\dagger(\downarrow)n_R^\dagger(\uparrow)]|0\rangle, \tag{2.7}$$

where $N(\mu)$ is a normalization factor. As $\mu$ varies from 0 to 1 the state thus formed describes a one-parameter path through configuration space which characterizes the separation of two nucleons. Because of the antisymmetrization of the state (implicit in the fermion-operator notation), the identification of the configuration with the two-nucleon channel is unambiguous only when $\mu=1$ and the right and left orbitals are orthogonal. Similar constructions can, of course, be carried out for other two-baryon combinations which communicate with the desired channel. More general configurations which include admixtures of these states are not considered here.

The even- (odd-) parity channels have even (odd) numbers of quarks in $P$ orbitals. At $\mu=0$ the even-parity channels have all quarks in the $S_{1/2}$ orbital and the odd-parity channels have five in the $S_{1/2}$ and one in the $P_{3/2}$ orbital.[12] For general $\mu$ the configurations are not eigenstates of total angular momentum $J$. It is tedious but straightforward to project out states of definite $J$ for the spherical cavity, but this has not been done here for the sake of simplicity. The expectation value
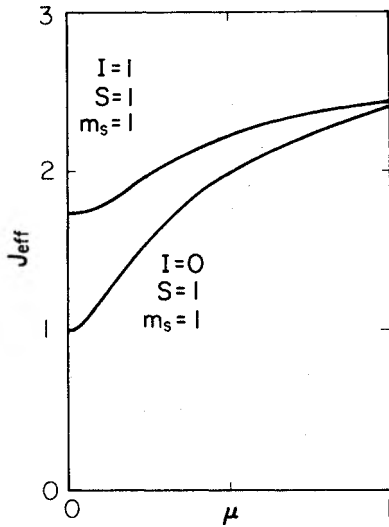
FIG. 2. Effective cavity angular momentum defined by $J_{\text{eff}}(J_{\text{eff}}+1) = \langle J^2 \rangle$ for two configurations as a function of the orbital mixing parameter $\mu$.



FIG. 3. Diagrams representing terms in the effective Hamiltonian.

$\langle J^2 \rangle$ for the cavity as a function of $\mu$ for two states is shown in Fig. 2, computed as described in Appendix B. It is expected than an increased kinetic energy of rotation at higher $\langle J^2 \rangle$ will raise the deformation energy computed with the configurations (2.7) compared with the deformation energy for a state of a definite lowest value of $J$. Since $\mu$ increases with separation, the curves at larger separation will be distorted, but at small values of $\mu$ this effect is unimportant.

The kinetic energy of the quarks in the cavity of radius $R$ is given by

$$E_Q = [n_S(\mu)\omega_S + n_P(\mu)\omega_P]/R ,\qquad (2.8)$$

where $n_S(\mu)$ and $n_P(\mu)$ are the average numbers of quarks in the $S$ and $P$ orbitals, computed as described in Appendix B. The cavity eigenenergy for the $P$ orbital includes, of course, the rotational energy of that level. Thus the kinetic energy $E_Q$ includes a centrifugal-barrier term for the odd-parity channels (which have the lowest two-baryon orbital angular momentum $L = 1$.) However, our baryons are formed from quarks in the lowest cavity eigenmodes and so have an imprecise center-of-mass position. Thus it is not possible to achieve a precise zero separation of the centers of mass and no infinite centrifugal repulsion appears.

### B. Gluon terms

The interaction energy for the quarks in a given configuration is computed to second order in the color coupling constant. The procedure is detailed
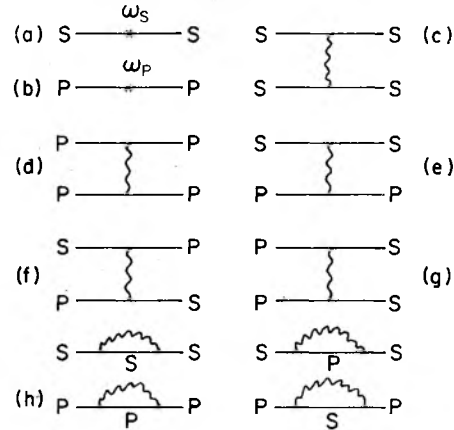
in Refs. 9 and 10. Basically what is required is to evaluate the expectation value of

$$H_G = \int dV\{\tfrac{1}{2}[(\vec{E}^a)^2 + (\vec{B}^a)^2] - \vec{J}^a \cdot \vec{A}^a\} , \qquad (2.9)$$

where the color-electrostatic fields are derived from the quark current

$$J_\mu^a = g:\bar{q}\lambda^a\gamma_\mu q: \qquad (2.10)$$

by solving Maxwell's equations

$$\nabla \cdot \vec{E}^a = J^{0a}, \quad \nabla \times \vec{B}^a = J^a, \quad r < R^\bullet \qquad (2.11)$$

with the bag boundary condition

$$\hat{r} \cdot \vec{E}^a = 0, \quad \hat{r} \times \vec{B}^a = 0, \quad r = R . \qquad (2.12)$$

The relevant part of the quark field is

TABLE I. (a) Values of reduced gluon multipole energies for the unit sphere and (b) values of terms appearing in the field energy for the unit sphere with $\alpha = 0.54$.

| (a) | | | | | |
|---|---|---|---|---|---|
| $W_{SM1}$ | $-0.176\alpha$ | $W_{E2}$ | $0.108\alpha$ | $W_{X01}$ | $0.430\alpha$ |
| $W_{PM1}$ | $-0.335\alpha$ | $W_{E0}$ | $0.011\alpha$ | $W_{XE1}$ | $-0.008\alpha$ |
| $W_{PM3}$ | $-0.067\alpha$ | $W_{SPM1}$ | $0.255\alpha$ | $W_{XM2}$ | $-0.094\alpha$ |

| (b) | | | |
|---|---|---|---|
| $W_{MSz}$ | $-0.0475$ | $W_{MX\perp}$ | $-0.020$ |
| $W_{MS\perp}$ | $-0.0475$ | $W_{EX\perp}$ | $0.029$ |
| $W_{MPz}$ | $-0.025$ | $W_{MXz}$ | $-0.0253$ |
| $W_{MP\perp}$ | $-0.047$ | $W_{EXz}$ | $0.0$ |
| $W_{MSPz}$ | $-0.022$ | $W_{MX}$ | $-0.002$ |
| $W_{MSP\perp}$ | $-0.044$ | $W_{EX}$ | $0.116$ |
| $W_{ED}$ | $0.020$ | $E_{\text{self}}$ | $0.0$ |
| $\omega_S$ | $2.043$ | | |
| $\omega_P$ | $3.204$ | | |

$$q = \sum_{c,f,m} (q_{Scfm} b_{Scfm} + q_{Pcfm} b_{Pcfm}) . \qquad (2.13)$$

Thus the fields are bilinear in the quark creation and annihilation operators and the interaction terms $H_G$ are at most quadrilinear in these opera-

tors. The several resulting contributions to the energy together with the fermion kinetic energy are represented pictorially in Fig. 3. The total field energy exclusive of the zero-point energy is summarized by the following expression [See (2.12) of Ref. 10]:

$$RE_F = n_S \omega_S + n_P \omega_P + (W_{MSz} C_{Sz} + W_{MS\perp} C_{S\perp}) + (W_{MPz} C_{Pz} + W_{MP\perp} C_{P\perp}) + (W_{MSPz} C_{SPz} + W_{MSP\perp} C_{SP\perp} + W_{ED} C_D)$$
$$+ [W_{MX\perp} + W_{EX\perp}) C_{X\perp d} + (W_{MXz} + W_{EXz}) C_{Xzd} + (W_{EX} + W_{MX}) C_{Xd}]$$
$$+ [(W_{MX\perp} - W_{EX\perp}) C_{X\perp 0} + (W_{MXz} - W_{EXz}) C_{Xz0} + (W_{EX} - W_{MX}) C_{X0}] . \qquad (2.14)$$

The seven terms have been grouped in order so as to correspond to the first seven diagrams of Fig. 3. The self-energy contribution of Fig. 3(h) is treated the same way as in Ref. 8. A general description of the terms in (2.14) follows. The subscripted factors $W$ are basic configuration-independent gluon interaction energies. They are constructed by solving Maxwell's equations for the $c$-number quark currents formed from the various orbitals and substituting the resulting fields into expressions for the field energy. For example, the current

$$\vec{J}_{SS} = g q_S^\dagger \vec{\alpha} q_S \qquad (2.15)$$

gives rise to the field $\vec{B}_{SS}$ which satisfies

$$\nabla \times \vec{B}_{SS} = \vec{J}_{SS} \qquad (2.16)$$

and the term $W_{MS}$ through

$$\int [\tfrac{1}{2}(\vec{B}_{SS})^2 - \vec{J}_{SS} \cdot \vec{A}_{SS}] dV = W_{MSz} \sigma_1^3 \sigma_2^3 + W_{MS\perp} \vec{\sigma}_1^\perp \cdot \vec{\sigma}_2^\perp , \qquad (2.17)$$

where $\vec{\sigma}_1$ and $\vec{\sigma}_2$ give the spin coupling at the upper and lower vertex of Fig. 3(a). The values of the various terms for the sphere are given in Table I and Appendix A. The subscripted coefficients $C$ and $n$ are configuration-dependent and rise from the evaluation of the expectation value on the given state of the combination of quark creation and annihilation operators implied by the diagrams of Fig. 3. Thus, for example,

$$C_{Sz}(\mu) = \sum_a \langle : b_S^\dagger \sigma^3 \lambda^a b_S b_S^\dagger \sigma^3 \lambda^a b_S : \rangle . \qquad (2.18)$$

Here color and flavor indices have been suppressed. The values of the coefficients $C$ for the various channels are given in Appendix B and Table II.

## C. Deformation energy

The energy of the bag for a given configuration is found by minimizing with respect to $R$ expression

$$E(\mu,R) = E_F(\mu,R) + E_0(R) + \tfrac{4\pi}{3} R^3 B , \qquad (2.19)$$

where the quark and gluon energy $E_F$ is given by (2.14) and the zero-point energy is

$$E_0(R) = -Z_0/R , \qquad (2.20)$$

where $Z_0 = 1.84$ has been chosen to give the correct masses for the $\rho$, $N$, and $\Delta$.[8] From the point of view of the static cavity approximation the stable configuration is the one which minimizes $E$ with respect to both $\mu$ and $R$. We find that in all two-nucleon channels, the overall stable minimum occurs for a finite value of $\mu$ between 0 and 1. This is the end of the story as far as the static cavity approximation is concerned; in all channels we find semiclassical stable six-quark states, consisting of two partially separated nucleons. However, one expects large quantum fluctuations in the two-nucleon c.m. coordinate just as in the conventional potential model of the two-nucleon interaction.

To study these fluctuations, it is necessary to go beyond the static cavity approximation. What is needed is a dynamical treatment of the collective motion of the system as a function of a few parameters which characterize the gross distortion of the system away from the point of semiclassical equilibrium. If the kinetic energies of the collective motion are small compared to the internal excitation energies, the motion may be treated adiabatically[13]—i.e., one allows the quark and gluon fields to adjust instantaneously to each small change in the collective coordinate. There are four steps leading to a full dynamical treatment of the collective motion. First, a collective

TABLE II. Configurations factors, two nucleons. (a) $I=0$, $S=1$, $m_S=1$ (cf. Appendix B). (b) $I=1$, $S=1$, $m_S=1$. (c) $I=0$, $S=1$, $m_S=0$. (d) $I=1$, $S=1$, $m_S=0$. (e) $I=1$, $S=0$. (f) $I=0$, $S=0$. The overbars indicate repeated digits. For example, $42.\overline{6}=42.666.\ldots$

**(a) $I=0$, $S=1$, $m_S=1$**

| | $\mu^0$ | $\mu^1$ | $\mu^2$ | $\mu^3$ | $\mu^4$ | $\mu^5$ | $\mu^6$ |
|---|---|---|---|---|---|---|---|
| $N$ | 5 | | 67 | | 67 | | 5 |
| $Nn_S$ | 30 | | 268 | | 134 | | 0 |
| $Nn_P$ | 0 | | 134 | | 268 | | 30 |
| $NC_{Sz}$ | $42.\overline{6}$ | | $298.\overline{6}$ | | $85.\overline{3}$ | | 0 |
| $NC_{S\perp}$ | $-69.\overline{3}$ | | $-202.\overline{6}$ | | $186.\overline{6}$ | | 0 |
| $NC_{Pz}$ | 0 | | $85.\overline{3}$ | | $298.\overline{6}$ | | $42.\overline{6}$ |
| $NC_{P\perp}$ | 0 | | $186.\overline{6}$ | | $-202.\overline{6}$ | | $-69.\overline{3}$ |
| $NC_{SPz}$ | 0 | | $341.\overline{3}$ | | $341.\overline{3}$ | | 0 |
| $NC_{SP\perp}$ | 0 | | $1621.\overline{3}$ | | $1621.\overline{3}$ | | 0 |
| $NC_D$ | 0 | | $597.\overline{3}$ | | $597.\overline{3}$ | | 0 |
| $NC_{Xzd}$ | 0 | | $426.\overline{6}$ | | $426.\overline{6}$ | | 0 |
| $NC_{X\perp d}$ | 0 | | $-85.\overline{3}$ | | $-85.\overline{3}$ | | 0 |
| $NC_{Xd}$ | 0 | | $-1109.\overline{3}$ | | $-1109.\overline{3}$ | | 0 |
| $NC_{Xz0}$ | | 128 | | $426.\overline{6}$ | | 128 | |
| $NC_{X\perp 0}$ | | $565.\overline{3}$ | | 2112 | | $565.\overline{3}$ | |
| $NC_{X0}$ | | $-320$ | | $-1749.\overline{3}$ | | $-320$ | |
| $NC_J$ | 10 | | 402 | | 702 | | 70 |

**(b) $I=1$, $S=1$, $m_S=1$**

| | $\mu^0$ | $\mu^1$ | $\mu^2$ | $\mu^3$ | $\mu^4$ |
|---|---|---|---|---|---|
| $N$ | $8.\overline{3}$ | | $55.\overline{3}$ | | $8.\overline{3}$ |
| $Nn_S$ | $41.\overline{6}$ | | 166 | | $8.\overline{3}$ |
| $Nn_P$ | $8.\overline{3}$ | | 166 | | $41.\overline{6}$ |
| $NC_{Sz}$ | $-49.\overline{7}$ | | $21.\overline{3}$ | | 0 |
| $NC_{S\perp}$ | $7.\overline{1}$ | | $177.\overline{7}$ | | 0 |
| $NC_{Pz}$ | 0 | | $21.\overline{3}$ | | $-49.\overline{7}$ |
| $NC_{P\perp}$ | 0 | | $177.\overline{7}$ | | $7.\overline{1}$ |
| $NC_{SPz}$ | $56.\overline{8}$ | | $711.\overline{1}$ | | $56.\overline{8}$ |
| $NC_{SP\perp}$ | $69.\overline{3}$ | | $1027.5$ | | $69.\overline{3}$ |
| $NC_D$ | $44.\overline{4}$ | | $266.\overline{6}$ | | $44.\overline{4}$ |
| $NC_{Xzd}$ | $-35.\overline{5}$ | | $14.\overline{2}$ | | $-35.\overline{5}$ |
| $NC_{X\perp d}$ | $-12.\overline{4}$ | | $394.\overline{6}$ | | $-12.\overline{4}$ |
| $NC_{Xd}$ | $-88.\overline{8}$ | | $-1415.\overline{1}$ | | $-88.\overline{8}$ |
| $NC_{Xz0}$ | | $412.\overline{4}$ | | $412.\overline{4}$ | |
| $NC_{X\perp 0}$ | | $583.\overline{1}$ | | $583.\overline{1}$ | |
| $NC_{X0}$ | | $-355.\overline{5}$ | | $-355.\overline{5}$ | |
| $NC_J$ | $39.\overline{6}$ | | $467.\overline{3}$ | | $95.\overline{6}$ |

TABLE II. *(Continued).*

(c) $I=0$, $S=1$, $m_S=0$

| | $\mu^0$ | $\mu^1$ | $\mu^2$ | $\mu^3$ | $\mu^4$ | $\mu^5$ | $\mu^6$ |
|---|---|---|---|---|---|---|---|
| $N$ | 5 | | 67 | | 67 | | 5 |
| $Nn_S$ | 30 | | 268 | | 134 | | 0 |
| $Nn_P$ | 0 | | 134 | | 268 | | 30 |
| $NC_{Sz}$ | $-112$ | | $-501.\overline{3}$ | | $101.\overline{3}$ | | 0 |
| $NC_{S\perp}$ | $85.\overline{3}$ | | $597.\overline{3}$ | | $170.\overline{6}$ | | 0 |
| $NC_{Pz}$ | 0 | | $101.\overline{3}$ | | $-501.\overline{3}$ | | $-112$ |
| $NC_{P\perp}$ | 0 | | $170.\overline{6}$ | | $597.\overline{3}$ | | $85.\overline{3}$ |
| $NC_{SPz}$ | 0 | | 1280 | | 1280 | | 0 |
| $NC_{SP\perp}$ | 0 | | $682.\overline{6}$ | | $682.\overline{6}$ | | 0 |
| $NC_D$ | 0 | | $597.\overline{3}$ | | $597.\overline{3}$ | | 0 |
| $NC_{Xzd}$ | 0 | | $-512$ | | $-512$ | | 0 |
| $NC_{X\perp d}$ | 0 | | $853.\overline{3}$ | | $853.\overline{3}$ | | 0 |
| $NC_{Xd}$ | 0 | | $-1109.\overline{3}$ | | $-1109.\overline{3}$ | | 0 |
| $NC_{Xz0}$ | | $437.\overline{3}$ | | $1685.\overline{3}$ | | $437.\overline{3}$ | |
| $NC_{X\perp 0}$ | | 256 | | $853.\overline{3}$ | | 256 | |
| $NC_{X0}$ | | $-320$ | | $-1749.\overline{3}$ | | $-320$ | |
| $NC_J$ | 10 | | 457 | | 856 | | 85 |

(d) $I=1$, $S=1$, $m_S=0$

| | $\mu^0$ | $\mu^1$ | $\mu^2$ | $\mu^3$ | $\mu^4$ |
|---|---|---|---|---|---|
| $N$ | $8.\overline{3}$ | | $55.\overline{3}$ | | $8.\overline{3}$ |
| $Nn_S$ | $41.\overline{6}$ | | 166 | | $8.\overline{3}$ |
| $Nn_P$ | $8.\overline{3}$ | | 166 | | $41.\overline{6}$ |
| $NC_{Sz}$ | $56.\overline{8}$ | | $156.\overline{4}$ | | 0 |
| $NC_{S\perp}$ | $-99.\overline{5}$ | | $42.\overline{6}$ | | 0 |
| $NC_{Pz}$ | 0 | | $156.\overline{4}$ | | $56.\overline{8}$ |
| $NC_{P\perp}$ | 0 | | $42.\overline{6}$ | | $-99.\overline{5}$ |
| $NC_{SPz}$ | $12.\overline{4}$ | | $316.\overline{4}$ | | $12.\overline{4}$ |
| $NC_{SP\perp}$ | $113.\overline{7}$ | | $1422.\overline{2}$ | | $113.\overline{7}$ |
| $NC_D$ | $44.\overline{4}$ | | $266.\overline{6}$ | | $44.\overline{4}$ |
| $NC_{Xzd}$ | $23.\overline{1}$ | | $380.\overline{4}$ | | $23.\overline{1}$ |
| $NC_{X\perp d}$ | $-71.\overline{1}$ | | $28.\overline{4}$ | | $-71.\overline{1}$ |
| $NC_{Xd}$ | $-88.\overline{8}$ | | $-1415.\overline{1}$ | | $-88.\overline{8}$ |
| $NC_{Xz0}$ | | $170.\overline{6}$ | | $170.\overline{6}$ | |
| $NC_{X\perp 0}$ | | $824.\overline{8}$ | | $824.\overline{8}$ | |
| $NC_{X0}$ | | $-355.\overline{5}$ | | $-355.\overline{5}$ | |
| $NC_J$ | 46 | | $527.\overline{3}$ | | 108 |

TABLE II. *(Continued)*.

(e) $I=1$, $S=0$

| | $\mu^0$ | $\mu^1$ | $\mu^2$ | $\mu^3$ | $\mu^4$ | $\mu^5$ | $\mu^6$ |
|---|---|---|---|---|---|---|---|
| $N$ | 5 | | 67 | | 67 | | 5 |
| $Nn_S$ | 30 | | 268 | | 134 | | 0 |
| $Nn_P$ | 0 | | 134 | | 268 | | 30 |
| $NC_{Sz}$ | $-26.\overline{6}$ | | $-103.\overline{1}$ | | $72.\overline{8}$ | | 0 |
| $NC_{S\perp}$ | $-53.\overline{3}$ | | $-206.\overline{2}$ | | $145.7$ | | 0 |
| $NC_{Pz}$ | 0 | | $72.\overline{8}$ | | $-103.\overline{1}$ | | $-26.\overline{6}$ |
| $NC_{P\perp}$ | 0 | | $145.7$ | | $-206.\overline{2}$ | | $-53.\overline{3}$ |
| $NC_{SPz}$ | 0 | | $824.\overline{8}$ | | $824.\overline{8}$ | | 0 |
| $NC_{SP\perp}$ | 0 | | $1649.7$ | | $1649.7$ | | 0 |
| $NC_D$ | 0 | | $597.\overline{3}$ | | $597.\overline{3}$ | | 0 |
| $NC_{Xzd}$ | 0 | | $-56.\overline{8}$ | | $-56.\overline{8}$ | | 0 |
| $NC_{X\perp d}$ | 0 | | $-113.\overline{7}$ | | $-113.\overline{7}$ | | 0 |
| $NC_{Xd}$ | 0 | | $-1109.\overline{3}$ | | $-1109.\overline{3}$ | | 0 |
| $NC_{Xz0}$ | | $266.\overline{6}$ | | $1116.\overline{4}$ | | $266.\overline{6}$ | |
| $NC_{X\perp 0}$ | | $533.\overline{3}$ | | $2232.\overline{8}$ | | $533.\overline{3}$ | |
| $NC_{X0}$ | | $-320$ | | $-1749.\overline{3}$ | | $-320$ | |
| $NC_J$ | 0 | | $334.\overline{3}$ | | $435.\overline{3}$ | | 45 |

(f) $I=0$, $S=0$

| | $\mu^0$ | $\mu^1$ | $\mu^2$ | $\mu^3$ | $\mu^4$ |
|---|---|---|---|---|---|
| $N$ | 1 | | 22 | | 1 |
| $Nn_S$ | 5 | | 66 | | 1 |
| $Nn_P$ | 1 | | 66 | | 5 |
| $NC_{Sz}$ | 0 | | $71.\overline{1}$ | | 0 |
| $NC_{S\perp}$ | 0 | | $142.\overline{2}$ | | 0 |
| $NC_{Pz}$ | 0 | | $71.\overline{1}$ | | 0 |
| $NC_{P\perp}$ | 0 | | $142.\overline{2}$ | | 0 |
| $NC_{SPz}$ | $-5.3$ | | $124.\overline{4}$ | | $-5.\overline{3}$ |
| $NC_{SP\perp}$ | $-10.\overline{6}$ | | $248.\overline{8}$ | | $-10.\overline{6}$ |
| $NC_D$ | $5.\overline{3}$ | | 32 | | $5.\overline{3}$ |
| $NC_{Xzd}$ | $-1.\overline{7}$ | | $145.7$ | | $-1.\overline{7}$ |
| $NC_{X\perp d}$ | $-3.\overline{5}$ | | $291.\overline{5}$ | | $-3.\overline{5}$ |
| $NC_{Xd}$ | $-10.\overline{6}$ | | $-661.\overline{3}$ | | $-10.\overline{6}$ |
| $NC_{Xz0}$ | | $56.\overline{8}$ | | $56.\overline{8}$ | |
| $NC_{X\perp 0}$ | | $113.\overline{7}$ | | $113.\overline{7}$ | |
| $NC_{X0}$ | | $-42.\overline{6}$ | | $-42.\overline{6}$ | |
| $NC_J$ | 2 | | $116.\overline{6}$ | | 8 |

variable or variables ($\delta$) are selected. Second, a deformation energy $V(\delta)$ is computed as a function of this variable. Third, one must find the kinetic energy $K(\delta,\dot{\delta})$ associated with small rates of variation of the collective variable. Finally, the effective Hamiltonian $K+V$ is quantized to obtain the wave function in the collective variable.

So far we have carried out only the first two steps of this program.

To some extent the choice of collective variables is arbitrary, provided they characterize a macroscopic property of the motion. Most arbitrariness is removed once the kinetic energy is known. For example, a change from a parameter $\delta$ to a func-

CARLETON DeTAR

tion of the parameter $f(\delta)$ results in a compensating change in the kinetic energy.

We have continued to use the variable of Refs. 9 and 10, namely

$$\delta = \frac{2\sqrt{\mu}(1+\mu)}{1+\mu^2} z_{SP},$$

$$z_{SP} = \int q_S^\dagger(\vec{r})q_P(\vec{r})z\,dV, \qquad (2.21)$$

which was motivated in Ref. 9 as a measure of the separation of the orbitals. Another choice with perhaps more dynamical significance would be a measure of the rms separation of two groups of three quarks using the baryon-number density as a probability measure. This is not a well-defined quantity since the antisymmetrization of the wave function mixes quarks among the orbitals. However, a rudimentary measure can be constructed by computing the expectation value of

$$\left(\frac{\vec{r}_1+\vec{r}_2+\vec{r}_3}{3}-\frac{\vec{r}_4+\vec{r}_5+\vec{r}_6}{3}\right)^2 \qquad (2.22)$$

on the ordered state

$$q(\vec{r}_1\cdots\vec{r}_6)=q_L(\vec{r}_1)q_L(\vec{r}_2)q_L(\vec{r}_3)q_R(\vec{r}_4)q_R(\vec{r}_5)q_R(\vec{r}_6),$$
$$\qquad (2.23)$$

where

$$(1+\mu)^{1/2}q_L(\vec{r})=q_S(\vec{r})-\sqrt{\mu}q_P(\vec{r}),$$
$$(1+\mu)^{1/2}q_R(\vec{r})=q_S(\vec{r})+\sqrt{\mu}q_P(\vec{r}). \qquad (2.24)$$

Thus we might use

$$\bar{r}^2 = \frac{6}{9}\frac{r_S^2+\mu r_P^2}{1+\mu}+\frac{30}{9}\frac{4\mu}{(1+\mu)^2}z_{SP}^2, \qquad (2.25)$$

where $z_{SP}$ is defined above (2.21) and

$$r_S^2 = \int q_S^\dagger q_S r^2 dV, \quad r_P^2 = \int q_P^\dagger q_P r^2 dV. \qquad (2.26)$$

For the sphere $r_S = 0.729\ R$, $r_P = 0.787\ R$, $z_{SP} = 0.342\ R$. In Fig. 4 a plot of $\bar{r}$ vs $\delta$ is shown for the state $I=0$, $S=1$, $m_S=1$. The separation rate in $\bar{r}$ is slower than that in $\delta$ for small separations, but they begin to approach each other in value at larger separations. The function $\bar{r}(\delta)$ depends weakly on the choice of channel since $R(\delta)$, the radius of the sphere, depends weakly on the channel.

The deformation energy is computed by calculating the energy of the bag constraining the collective variable. This is easily done using the method of Lagrange multipliers. One seeks a stationary value of the variational expression

$$I(R,\mu,\lambda)=E(\mu,R)-\lambda\delta(\mu,R) \qquad (2.27)$$

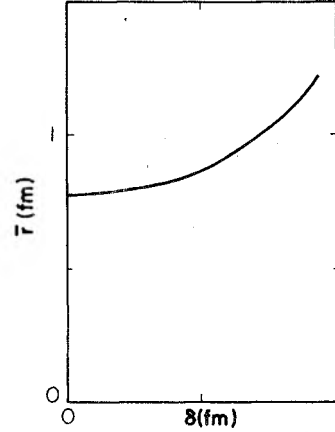with respect to variations in $R$ and $\mu$ with $\lambda$ fixed.



FIG. 4. Values of the rms separation $\bar{r}$ computed as a function of the constrained separation parameter $\delta$ for $I=0$, $S=1$, $m_S=1$.

The values of the energy and separation at the stationary points $E(\lambda)$ and $\delta(\lambda)$ define a point on the deformation energy curve. Because the energy (2.14), (2.19), and separation (2.21) have a simple dependence on $R$, the variational expression (2.27) may be written

$$I(R,\mu,\lambda)=c(\mu)/R+\tfrac{4\pi}{3}R^3B-\lambda d(\mu)R \qquad (2.28)$$

and the stationary points are given by the values of $\mu$ which satisfy

$$R^2(\mu)=c'(\mu)/\lambda d'(\mu)$$
$$=\frac{\lambda d(\mu)+[\lambda^2 d^2(\mu)+16\pi Bc(\mu)]^{1/2}}{8\pi B} \qquad (2.29)$$

for a given value of $\lambda$. Results of the computation are shown in Figs. 5(a) and 5(b) for the various channels. They are discussed in the following section.

III. DISCUSSION

The soft repulsive core seen in the even-parity channels [Fig. 5(a)] is more repulsive in the iso-triplet channel than in the isosinglet channel.[8] Whether the additional repulsion is sufficient to prevent the occurrence of a two-nucleon bound state in the isotriplet channel in accordance with experiment cannot be determined without a full dynamical calculation. However, the fact that a higher isotriplet energy is found throughout the entire range is reassuring. In the spin-triplet channel the deformation energy is found to be substantially higher in the state with $m_S=0$ along the separation axis compared with that of the $m_S=1$ state. In the conventional decomposition of the two-nucleon potential
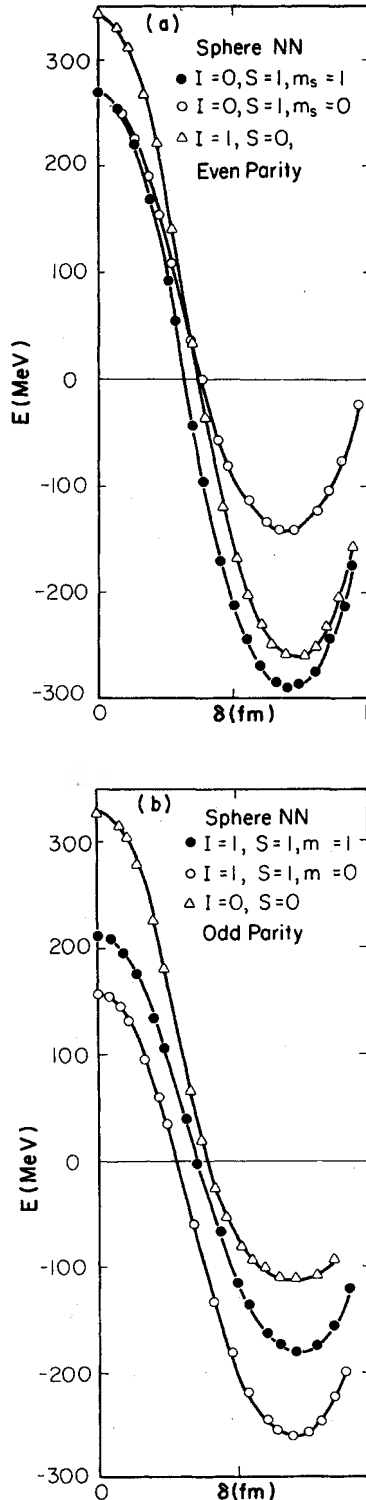
FIG. 5. Interaction energy for the two-nucleon config-
uration in a spherical bag as a function of the constrain-
ed separation parameter $\delta$ (a) for even-parity two-nucle-
on configurations, and (b) for odd-parity configurations
with rotational kinetic energy included.

$$V^I = V_c^I + V_S^I \vec{\sigma}_1 \cdot \vec{\sigma}_2 + V_T^I S_{12} + V_{SO}^I \vec{S} \cdot \vec{L}, \qquad (3.1)$$

where $\vec{\sigma}_1$ and $\vec{\sigma}_2$ are the nucleon spinors, $\vec{S}$ and $\vec{L}$
are the total nuclear spin and orbital angular mo-
mentum, and

$$S_{12} = 3\vec{\sigma}_1 \cdot \hat{r}_{12} \vec{\sigma}_2 \cdot \hat{r}_{12} - \vec{\sigma}_1 \cdot \vec{\sigma}_2 \qquad (3.2)$$

is the tensor operator (in our case $\hat{r}_{12} = \hat{z}$); the
difference between the curves for $m_S = 0$ and $m_S$
$= 1$ is simply proportional to the tensor interaction
energy. This is shown in Fig. 6 for both even-
and odd-parity channels. The sign of $V_T^{I=0}$ agrees
with that found in more conventional models.[14]
An attractive tensor term in the isosinglet channel
ensures the correct sign for the quadrupole mo-
ment of the deuteron. The sign of $V_T^{I=1}$ also agrees
with that of the Yale, Hamada–Johnston, and
Paris potentials.[14] It should be emphasized that a
more quantitative comparison between the bag de-
formation energies in Fig. 5 and 6 and standard
two-body potentials is not possible without a full
dynamical treatment of the collective motion,
particularly in view of the flexibility in defining
the separation parameter $\delta$. It is amusing that the
isosinglet tensor interaction vanishes at $\delta = 0$.
This follows simply from the rotational symmetry
of the $S = 1$ six-quark state with all quarks in the
$S_{1/2}$ orbital: It is an eigenstate of total $J = S = 1$.

It is tempting to try to isolate the spin-spin
component $V_S^I$ by subtracting an odd-parity curve
from an even-parity curve. Unfortunately, the
odd-parity curves include some effects of a cen-
trifugal barrier (See Sec. II A). Thus the term
$V_c^I$ in (3.1) must be regarded for the purposes of
our computation as having an $L$ dependence. The
collective rotational kinetic energy associated with
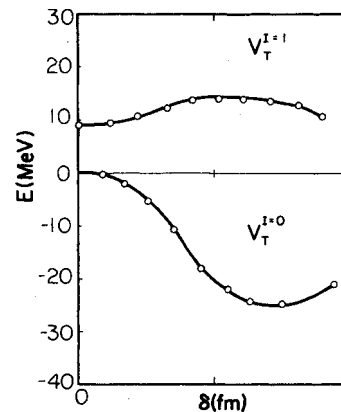the barrier need not have a simple $L^2/I(\delta)$ depen-



FIG. 6. Isotriplet and isosinglet tensor contributions
to the two-nucleon interaction energy derived from Fig.
5.

dence. Thus it may not be possible to isolate all of the terms in (3.1), except in some approximate sense.

There has been considerable interest recently in studying the two-nucleon interaction in the context of the nonrelativistic quark model.[15,16] This traditional model has a distinct advantage in ease of computation even if it is lacking in a fundamental theoretical justification. Liberman[15] has calculated the separation energy of two Gaussian clusters of three colored quarks. In his model interactions between pairs of quarks are given by a simple harmonic-oscillator potential, partially modified to correspond to a nonrelativistic reduction of a colored-vector-gluon exchange,[17]

$$V_{ij} = -\lambda_i \cdot \lambda_j \left[ v(r_{ij}) + \frac{1}{6} \left( \frac{\hbar}{M_Q c} \right)^2 \sigma_i \cdot \sigma_j \nabla^2 v(r_{ij}) \right], \quad (3.3)$$

where $v(r) = kr^2/2$. Since the associated spin-orbit and tensor terms are omitted, his calculation does not yield a tensor interaction. However, it is amusing that there are qualitative similarities between his results and ours. In both models in the even-parity channel, the isotriplet combination has a more repulsive core than the isosinglet. This effect is a consequence of the color-magnetic interaction between the quarks at short distances and depends only on the expectation value $\langle -\lambda_i \cdot \lambda_j \sigma_i \cdot \sigma_j \rangle$ in the two states—not on the details of the interaction. A greater repulsion in the odd-parity isosinglet channel compared with the isotriplet channel is also found in both models. Thus it is likely that the broad qualitative features of our results follow from the color-vector nature of the gluon interaction.

In detail the results differ. We find a strong attraction in all channels which results from two effects: a strong color-electrostatic attraction among three quarks forming a color singlet, and a geometrical effect. The latter effect lowers the energy when the boundary between two nucleons is removed, since the cavity eigenenergies are lowered when the fields occupy the larger region. This latter effect is not present in the nonrelativistic quark model. However, the color-electrostatic attraction is present. Although Liberman's computation did not give a negative potential in any channel (no deuteron), his results were based on a variational approach; it may be possible to do better with a more sophisticated trial wave function or a modification of the potential (3.3).

We should also mention a different approach to the nonrelativistic colored-quark model discussed in a recent note by Kislinger. He argues that a semirelativistic treatment of vector-gluon exchange gives the correct sign for the spin-orbit term in the two-nucleon interaction.[18] The calcu-

lation is based on a simplified treatment of the motion of the quarks within each nucleon, but the result is amusing and the method deserves further study and refinement.

In conclusion, we have shown that the deformation energy of the two-nucleon system in the MIT bag model in configurations of various spins and isospins shows a number of qualitatively desirable features. In particular, the two-nucleon tensor interaction has the proper sign. The even-parity isotriplet channel is uniformly more repulsive than the even-parity isosinglet channel.

A number of important questions remain to be investigated. Obviously, an understanding of the dynamics of the collective motion would permit a more quantitative treatment of the interaction. Following the same approach described in the present work, other two-baryon channels may be studied for indications of states bound with respect to higher channels. Adiabatic mixing between the $\Delta\Delta$ channel and the $NN$ channel can be examined. This study is of interest in determining the amount of a $\Delta\Delta$ component present at short range in the deuteron.[19]

## APPENDIX A: GLUON-INTERACTION TERMS IN THE UNIT SPHERE

### 1. Diagonal fields

For the sake of completeness we review the evaluation of the various gluon-interaction terms in (2.14). There are three currents required:

$$J^\mu_{SS} = g\bar{q}_S \gamma_\mu q_S ,$$
$$J^\mu_{PP} = g\bar{q}_P \gamma_\mu q_P , \quad (A1)$$
$$J^\mu_{SP} e^{-i\omega t} = g\bar{q}_S \gamma_\mu q_P ,$$

where the fermion spinors are defined in (2.2). The color dependence is given by an overall factor of $\lambda^a$, which has been omitted. The currents $J^\mu_{SS}$ and $J^\mu_{PP}$ are static, but the transition current has a frequency $\omega = \omega_P - \omega_S$. The field energy is to be calculated in the approximation of degenerate second-order perturbation theory,[9] i.e., for $\omega^2 \ll \omega_0^2$ where $\omega_0$ is the lowest relevant gluon eigenfrequency. However, for the purposes of evaluating the fields associated with the $S$-$P$ transition it is convenient to solve the time-dependent Maxwell equations. Thus we must solve the static equations

$$\nabla^2 \vec{A}_{SS} = -\vec{J}_{SS}, \quad \nabla \times \vec{A}_{SS} = \vec{B}_{SS},$$

$$\nabla^2 \vec{A}_{PP} = -\vec{J}_{PP}, \quad \nabla \times \vec{A}_{PP} = \vec{B}_{PP}, \quad \text{(A2)}$$

$$\nabla^2 \phi_D = -J^0_{SS} + J^0_{PP}, \quad -\nabla \phi_D = \vec{E}_D$$

and the frequency-dependent equations

$$(\nabla^2 + \omega^2)\vec{A}_{SP} = -\vec{J}_{SP}, \quad \nabla \times \vec{A}_{SP} = \vec{B}_{SP},$$

$$\qquad\qquad\qquad\qquad\qquad\qquad\qquad\qquad \text{(A3)}$$

$$(\nabla^2 + \omega^2)\phi_{SP} = -J^0_{SP}, \quad -\nabla \phi_{SP} + i\omega \vec{A}_{SP} = \vec{E}_{SP}$$

with boundary conditions at $r = R = 1$,

$$\hat{r} \times \vec{B}_{SS} = \hat{r} \times \vec{B}_{PP} = \hat{r} \times \vec{B}_{SP} = 0,$$

$$\qquad\qquad\qquad\qquad\qquad\qquad\qquad \text{(A4)}$$

$$\hat{r} \cdot \vec{E}_D = \hat{r} \cdot \vec{E}_{SP} = 0.$$

(Only the difference between the $S$-state and $P$-state charge densities enters the computation because the state is a color singlet.[9])

The diagonal currents and charge densities have the form[9]

$$\vec{J}_{SS} = \vec{r} \times \nabla[j_{1S}(\vec{\sigma} \cdot \vec{r})],$$

$$\vec{J}_{PP} = \vec{r} \times \nabla[j_{3P}(\vec{\sigma} \cdot \vec{r}z^2 - \tfrac{2}{5}z\sigma^3 r^2 - \tfrac{1}{5}\vec{\sigma} \cdot \vec{r})$$

$$\qquad\qquad + j_{1P}(\sigma^3 z - 2\vec{\sigma} \cdot \vec{r})], \quad \text{(A5)}$$

$$J^0_{SS} - J^0_{PP} = \rho_0 + \rho_2(\tfrac{3}{2}z^2 - \tfrac{1}{2}r^2),$$

where the scalar functions $j_{1S}$, $j_{1P}$, $j_{3P}$, $\rho_0$, and $\rho_2$ can be found by a straightforward computation from (A1) (See Ref. 9). The magnetic dipole and octupole and electric monopole and quadrupole decomposition is explicit in (A5), and (A3) can be integrated numerically by standard techniques. The dependence of the fields upon the quark spins permits a net spin-flip or -nonflip contribution to the expectation value of the second-order terms of the type (2.17). Rotational symmetry relates the spin-flip and -nonflip contributions to the energy from each multipole term. Therefore the gluon interaction energies $W$ in (2.14) can be expressed entirely in terms of "reduced multipole energies".[9] Thus in (2.17)

$$W_{MSz} = |\langle 10 | \tfrac{1}{2}\tfrac{1}{2}; \tfrac{1}{2} - \tfrac{1}{2}\rangle|^2 W_{SM1},$$

$$\qquad\qquad\qquad\qquad\qquad\qquad\qquad \text{(A6)}$$

$$W_{MS\perp} = \tfrac{1}{2}|\langle 11 | \tfrac{1}{2}\tfrac{1}{2}, \tfrac{1}{2}\tfrac{1}{2}\rangle|^2 W_{SM1}.$$

In analogy with (2.17) we define

$$\tfrac{1}{2}\int (\vec{B}_{PP} \cdot \vec{B}_{PP} - \vec{J}_{PP} \cdot \vec{A}_{PP})dV = W_{MPz}\sigma_1^3\sigma_2^3 + W_{MP\perp}\vec{\sigma}_1^\perp \cdot \vec{\sigma}_2^\perp,$$

$$\tfrac{1}{2}\int (\vec{B}_{SS} \cdot \vec{B}_{PP} - \vec{J}_{SS} \cdot \vec{A}_{PP})dV = W_{MSPz}\sigma_1^3\sigma_2^3 + W_{MSP\perp}\vec{\sigma}_1^\perp \cdot \vec{\sigma}_2^\perp, \quad \text{(A7)}$$

$$\tfrac{1}{2}\int E_D^2 dV = W_{ED}.$$

The relationship to the reduced multipole energies is given by

$$W_{MPz} = |\langle 10 | \tfrac{3}{2}\tfrac{1}{2}, \tfrac{3}{2} - \tfrac{1}{2}\rangle|^2 W_{PM1}$$

$$\qquad + |\langle 30 | \tfrac{3}{2}\tfrac{1}{2}, \tfrac{3}{2} - \tfrac{1}{2}\rangle|^2 W_{PM3},$$

$$W_{MP\perp} = \tfrac{1}{2}|\langle 11 | \tfrac{3}{2}\tfrac{1}{2}, \tfrac{3}{2}\tfrac{1}{2}\rangle|^2 W_{PM1}$$

$$\qquad + \tfrac{1}{2}|\langle 31 | \tfrac{3}{2}\tfrac{1}{2}, \tfrac{3}{2}\tfrac{1}{2}\rangle|^2 W_{PM3},$$

$$W_{MSPz} = \langle 10 | \tfrac{3}{2}\tfrac{1}{2}, \tfrac{3}{2} - \tfrac{1}{2}\rangle$$

$$\qquad \times \langle \tfrac{1}{2}\tfrac{1}{2}, \tfrac{1}{2} - \tfrac{1}{2} | 10\rangle W_{SPM1}, \quad \text{(A8)}$$

$$W_{MSP\perp} = \tfrac{1}{2}\langle 11 | \tfrac{3}{2}\tfrac{1}{2}, \tfrac{3}{2}\tfrac{1}{2}\rangle\langle \tfrac{1}{2}\tfrac{1}{2}\tfrac{1}{2}\tfrac{1}{2} | 11\rangle W_{SPM1},$$

$$W_{ED} = |\langle 20 | \tfrac{3}{2}\tfrac{1}{2}, \tfrac{3}{2} - \tfrac{1}{2}\rangle|^2 W_{E2} + W_{E0}.$$

The values of the reduced multipole energies are given in Table I.

### 2. Transition fields

The (off-diagonal) transition currents and charge density have the form

$$\vec{J}_{SP} = i\psi(z\vec{r} - \tfrac{1}{3}r^2\vec{\sigma}\sigma^3) + i\phi(\vec{r}\vec{\sigma} \cdot \vec{r} - r^2\vec{\sigma})\sigma^3 + \tau z\vec{\sigma} \times \vec{r},$$

$$J^0_{SP} = \zeta(z - \tfrac{1}{3}\vec{\sigma} \cdot \vec{r}\sigma^3), \quad \text{(A9)}$$

where the terms in the real functions $\psi$, $\phi$, and $\zeta$ generate longitudinal and transverse electric dipole fields and the term in $\tau$ generates a magnetic quadrupole field. The solution of (A3) has the form

$$\vec{A} = \vec{A}^{(0)} + \vec{A}^{(E)} + \vec{A}^{(M)},$$

$$\qquad\qquad\qquad\qquad\qquad\qquad \text{(A10)}$$

$$\phi = \phi^{(0)},$$

where the longitudinal and transverse fields are given in the covariant gauge by

$$\mathbf{A}^{(0)} = -\sum_n \frac{i\alpha_{1n}^{(0)}\omega}{(\omega_{1n}^0)^2} \nabla j_1(\omega_{1n}^0 r)(z/r - \tfrac{1}{3}\sigma \cdot \hat{r}\sigma^3),$$

$$\phi^{(0)} = \sum_n \alpha_{1n}^{(0)} j_1(\omega_{1n}^0 r)(z/r - \tfrac{1}{3}\sigma \cdot \hat{r}\sigma^3),$$

$$\mathbf{A}^{(E)} = \sum_n i\alpha_{1n}^{(E)} \nabla \times j_1(\omega_{1n}^E r)\vec{\mathbf{X}}_1,$$ 
(A11)

$$\mathbf{A}^{(M)} = \sum_n \alpha_{2n}^{(M)} j_2(\omega_{2n}^M r)\vec{\mathbf{X}}_2,$$

and where the vector spherical harmonics are

$$\vec{\mathbf{X}}_1 = \hat{r}x\nabla(z/r - \tfrac{1}{3}\sigma \cdot r\sigma^3),$$
$$\vec{\mathbf{X}}_2 = \hat{r}x\nabla(3\sigma \cdot rz/r - \sigma^3),$$ 
(A12)

and the gluon eigenfrequencies are determined by

$$j_1'(\omega_{1n}) = 0, \quad j_1(\omega_{1n}^E) = 0, \quad \frac{d}{dr}[rj_2(\omega_{2n}^M r)] = 0. \quad \text{(A13)}$$

Equations (A3) are readily solved. The resulting fields contribute to the two interaction terms depicted in Figs. 3(f) and 3(g). The interaction energy contributed by the orbital-preserving term [Fig. 3(f)] can be shown to be

$$W_X = \tfrac{1}{2} \int (J_{SP}^{0\dagger}\phi_{SP} - \vec{\mathbf{J}}_{SP}^\dagger \cdot A_{SP})dV$$
$$= \tfrac{1}{2} \int (\vec{\mathbf{E}}_{SP}^\dagger \cdot \vec{\mathbf{E}}_{SP} - \vec{\mathbf{B}}_{SP}^\dagger \cdot \vec{\mathbf{B}}_{SP})dV. \quad \text{(A14)}$$

The orbital changing (off-diagonal) term [Fig. 3(g)] contributes

$$W_X' = \tfrac{1}{2}\text{Re} \int (J_{SP}^0\phi_{SP} - \vec{\mathbf{J}}_{SP} \cdot \vec{\mathbf{A}}_{SP})dV. \quad \text{(A15)}$$

It is necessary to interpret the phases of $J_{SP}^\mu$ carefully in (A15). In the spirit of degenerate second-order perturbation theory, the frequency $\omega = \omega_p - \omega_s$ is ignored compared with the gluon eigenfrequencies.[9] Thus the intrinsic time dependence of the current $J_{SP}^\mu$ and therefore the expression (A15) is ignored. The reality of $\psi$, $\phi$, $\tau$, and $\zeta$ in (A9) follows from the phase at $t = 0$ of the quark eigenfunctions (2.2), which is dictated by the left-right convention in (2.1). The remaining difficulty with (A15) lies in its apparent gauge dependence. A simple calculation shows that

$$W_X' = \tfrac{1}{2}\text{Re} \int (\vec{\mathbf{E}}_{SP} \cdot \vec{\mathbf{E}}_{SP} - \vec{\mathbf{B}}_{SP} \cdot \vec{\mathbf{B}}_{SP} - 2i\omega\vec{\mathbf{E}}_{SP} \cdot \vec{\mathbf{A}}_{SP}).$$
(A16)

Thus the gauge-dependent terms vanish as $\omega \to 0$. For convenience we have simply dropped the last

term. Direct calculation in the gauge $\hat{r} \cdot \vec{\mathbf{A}} = 0$ shows that the last term contributes less than 10% to $W_X'$. In the same spirit a further approximation can be made. The contributions to $W_X$ and $W_X'$ can be classified according to transverse and longitudinal multipole moments. The longitudinal moments contribute only to the electric field. The transverse moments contribute to both electric and magnetic fields, of course, but these electric fields are smaller by a factor of $\omega/\omega_0$ where $\omega_0$ is the lowest gluon eigenfrequency for the mode. Thus the contributions of the transverse fields to $\vec{\mathbf{E}}_{SP}^2$ in (A16) are negligible (approximately 10%). Finally, one may classify the Hermitian and anti-Hermitian terms in $\vec{\mathbf{E}}_{SP}$ and $\vec{\mathbf{B}}_{SP}$ by inspecting (A9). We find we may write

$$W_X = (W_{EX} + W_{MX}) + (W_{EX\varepsilon} + W_{MX\varepsilon})\sigma_1^3\sigma_2^3$$
$$+ (W_{EX\perp} + W_{MX\perp})\vec{\sigma}_1^\perp \cdot \vec{\sigma}_2^\perp,$$
(A17)

$$W_X' = (W_{EX} - W_{MX}) + (-W_{EX\varepsilon} + W_{MX\varepsilon})\sigma_1^3\sigma_2^3$$
$$+ (-W_{EX\perp} + W_{MX\perp})\vec{\sigma}_1^\perp \cdot \vec{\sigma}_2^\perp,$$

where the subscripts $E$ $(M)$ distinguish contributions from electric (magnetic) fields in (A14). In terms of multipole moments

$$W_{EX} = W_{1,0}^{(0)}, \quad W_{EX\varepsilon} \approx 0, \quad W_{EX\perp} = W_{11}^{(0)},$$
$$W_{MX} = W_{1,0}^{(E)}, \quad W_{MX\varepsilon} = W_{20}^{(M)}, \quad W_{MX\perp} = W_{21}^{(M)},$$
(A18)

and

$$W_{1,0}^{(E)} = |\langle \tfrac{3}{2}\tfrac{1}{2}\tfrac{1}{2} - \tfrac{1}{2} | 10 \rangle|^2 W_{XE1},$$

$$W_{1,0}^{(0)} = |\langle \tfrac{3}{2}\tfrac{1}{2}\tfrac{1}{2} - \tfrac{1}{2} | 10 \rangle|^2 W_{X01},$$

$$W_{1,1}^{(E)} = \tfrac{1}{2} |\langle \tfrac{3}{2}\tfrac{1}{2}\tfrac{1}{2}\tfrac{1}{2} | 11 \rangle|^2 W_{XE1},$$

$$W_{1,1}^{(1)} = \tfrac{1}{2} |\langle \tfrac{3}{2}\tfrac{1}{2}\tfrac{1}{2}\tfrac{1}{2} | 11 \rangle|^2 W_{X01},$$
(A19)

$$W_{2,0}^{(M)} = |\langle \tfrac{3}{2}\tfrac{1}{2}\tfrac{1}{2} - \tfrac{1}{2} | 20 \rangle|^2 W_{XM2},$$

$$W_{2,1}^{(M)} = \tfrac{1}{2} |\langle \tfrac{3}{2}\tfrac{1}{2}\tfrac{1}{2}\tfrac{1}{2} | 21 \rangle|^2 W_{XM2}.$$

The values of these terms are given in Table I.

## APPENDIX B: INTERNAL-SYMMETRY FACTORS FOR THE TWO-NUCLEON SYSTEM

### 1. Configuration factors

Given the normalized, antisymmetrized states of the form (2.7) which characterize the separation of two clusters of three quarks forming two

nucleons, as the parameter $\mu$ varies from 0 to 1, we wish to evaluate the expectation values of the configuration factors[10]

$$n_S = \langle b_S^\dagger b_S \rangle, \quad n_P = \langle b_P^\dagger b_P \rangle,$$

$$C_{S\parallel} = \langle : b_S^\dagger \sigma^3 \lambda^a b_S b_S^\dagger \sigma^3 \lambda^a b_S : \rangle,$$

$$C_{S\perp} = \langle : b_S^\dagger \vec{\sigma}_\perp \lambda^a b_S \cdot b_S^\dagger \vec{\sigma}^\perp \lambda^a b_S : \rangle,$$

$$C_{P\parallel} = \langle : b_P^\dagger \sigma^3 \lambda^a b_P b_P^\dagger \sigma^3 \lambda^a b_P : \rangle,$$

$$C_{P\perp} = \langle : b_P^\dagger \vec{\sigma}^\perp \lambda^a b_P \circ b_P^\dagger \vec{\sigma}^\perp \lambda^a b_P : \rangle,$$

$$C_{SP\parallel} = 2\langle : b_P^\dagger \sigma^3 \lambda^a b_P b_S^\dagger \sigma^3 \lambda^a b_S : \rangle,$$

$$C_{SP\perp} = 2\langle : b_P^\dagger \vec{\sigma}^\perp \lambda^a b_P \cdot b_S^\dagger \vec{\sigma}^\perp \lambda^a b_S : \rangle, \qquad (B1)$$

$$C_{X\parallel d} = 2\langle : b_P^\dagger \sigma^3 \lambda^a b_S b_S^\dagger \sigma^3 \lambda^a b_P : \rangle,$$

$$C_{X\perp d} = 2\langle : b_P^\dagger \vec{\sigma}^\perp \lambda^a b_S \cdot b_S^\dagger \vec{\sigma}^\perp \lambda^a b_P : \rangle,$$

$$C_{Xd} = 2\langle : b_P^\dagger \lambda^a b_S b_S^\dagger \lambda^a b_P : \rangle,$$

$$C_{X\parallel 0} = 2\langle : b_P^\dagger \sigma^3 \lambda^a b_S b_P^\dagger \sigma^3 \lambda^a b_S : \rangle,$$

$$C_{X\perp 0} = 2\langle : b_P^\dagger \vec{\sigma}^\perp \lambda^a b_S b_P^\dagger \vec{\sigma}^\perp \lambda^a b_S : \rangle,$$

$$C_{X0} = 2\langle : b_P^\dagger \lambda^a b_S b_P^\dagger \lambda^a b_S : \rangle,$$

$$C_D = -\langle : b_S^\dagger \lambda^a b_S b_P^\dagger \lambda^a b_P : \rangle.$$

Notice that the calculation of these expectation values is a bookkeeping problem which is entirely independent of the specific model for the colored six-quark system or the spherical geometry. These factors are also needed in the nonrelativistic colored quark model, for example, where the orthonormal states $S$ and $P$ are replaced by even and odd linear combinations of right and left orbitals. Since no simple and direct analytic procedure for evaluating all of these coefficients is known, a computer was used. The method has already been described briefly in Ref. 10; it has been extended to include all of the even- and odd-

parity two-nucleon channels.

The results for all channels are summarized in Table II. Each row of Table II defines a polynomial in $\mu$, the coefficients of which are given in the appropriate column. E.g., for the channel $I = 0$, $S = 1$, $m_S = 1$ the normalization polynomial $N$ is

$$N \equiv 5 + 67(\mu^2 + \mu^4) + 5\mu^6$$

and $\qquad\qquad\qquad\qquad\qquad (B2)$

$$C_{S\parallel} = (42\tfrac{2}{3} + 298\tfrac{2}{3}\mu^2 + 85\tfrac{1}{3}\mu^4)/N .$$

### 2. Angular momentum

The states (2.7) are not in general eigenstates of the total angular momentum. The expectation value of the total cavity angular momentum

$$J^2 = \left(\sum_{i=1}^{6} \vec{J}_i\right)^2 \qquad (B3)$$

is readily computed in terms of the expectation values of the same fundamental operators that entered into the computation of the configuration factors above.[10] The effect of the operator $\vec{J}_i \cdot \vec{J}_j$ upon a pair of quarks depends upon the orbital assignments of the quarks $i$ and $j$. If they are both $P$ quarks

$$\vec{J}_i \cdot \vec{J}_j = -1 - \tfrac{3}{4}\sigma_i^3 \sigma_j^3 + 2P_{ij}^\sigma ,$$

where the operator $P_{ij}^\sigma$ permutes the spin assignments of the quarks. If they are both $S$ quarks

$$\vec{J}_i \cdot \vec{J}_j = -\tfrac{1}{4} + \tfrac{1}{2}P_{ij}^\sigma , \qquad (B5)$$

and if one is $P$ and one $S$

$$\vec{J}_i \cdot \vec{J}_j = -\tfrac{1}{2} - \tfrac{1}{4}\sigma_i^3 \sigma_j^3 + P_{ij}^\sigma . \qquad (B6)$$

Thus

$$C_J(\mu) \equiv \langle J^2 \rangle = \tfrac{3}{4}\langle b_S^\dagger b_S \rangle + \tfrac{15}{4}\langle b_P^\dagger b_P \rangle - \langle : b_P^\dagger b_P b_P^\dagger b_P : \rangle - \tfrac{3}{4}\langle : b_P^\dagger \sigma^3 b_P b_P^\dagger \sigma^3 b_P : \rangle$$

$$+ 2\langle : b_P^\dagger b_P P_{12}^\sigma b_P^\dagger b_P : \rangle - \langle : b_P^\dagger b_P b_S^\dagger b_S : \rangle - \tfrac{1}{2}\langle : b_P^\dagger \sigma^3 b_P b_S^\dagger \sigma^3 b_S : \rangle + 2\langle : b_P^\dagger b_P P_{12}^\sigma b_S^\dagger b_S : \rangle$$

$$- \tfrac{1}{4}\langle : b_S^\dagger b_S b_S^\dagger b_S : \rangle + \tfrac{1}{2}\langle : b_S^\dagger b_S P_{12}^\sigma b_S^\dagger b_S : \rangle . \qquad (B7)$$

The expression for $C_J(\mu)$ is also represented in Table II for each channel.

[1]A. Chodos, R. L. Jaffe, K. Johnson, C. B. Thorn, and V. F. Weisskopf, Phys. Rev. D 9, 3471 (1974); A. Chodos, R. L. Jaffe, K. Johnson, and C. B. Thorn, ibid. 10, 2599 (1974).
[2]P. Hasenfratz and J. Kuti, Phys. Rep. 40C, 75 (1978).

[3]J. Kogut and L. Susskind, Phys. Rev. D 9, 3501 (1974).
[4]S. Mandelstam, Physics Rep. 23C, 245 (1976).
[5]C. Callan, R. Dashen, and D. Gross, Phys. Lett. 66B, 375 (1977); Phys. Rev. D 17, 2717 (1978); Princeton University reports, 1978 (unpublished).

[6]Charles Thorn, MIT Report No. MIT-CTP 722, 1978 (unpublished).

[7]T. D. Lee, Phys. Rev. D (to be published).

[8]T. DeGrand, R. L. Jaffe, K. Johnson, and J. Kiskis, Phys. Rev. D **12**, 2060 (1975).

[9]Carleton DeTar, Phys. Rev. D **17**, 302 (1978).

[10]Carleton DeTar Phys. Rev. D **17**, 323 (1978); **19**, 1028 (E) (1979).

[11]T. A. DeGrand and R. L. Jaffe, Ann. Phys. (NY) **100**, 425 (1976); T. A. DeGrand, *ibid.* **101**, 395 (1976).

[12]Spurious symmetric excitations of the six-quark c.m. coordinate inside the cavity do not occur in this configuration, since it must be odd under the interchange of left and right orbitals.

[13]The theory of adiabatic collective motion in nuclei is a good analogy. See, e.g., D. R. Inglis, Phys. Rev. **96**, 1059 (1954); **103**, 1786 (1956).

[14]See, for example, T. Hamada and I. D. Johnston, Nucl. Phys. **34**, 382 (1962); K. E. Lassila, M. H. Hull, M. Ruppel, F. A. McDonald, and G. Breit, Phys. Rev.

**126**, 881 (1962); R. Vinh Mau, in *Mesons in Nuclei*, edited by M. Rho and D. Wilkinson (North-Holland, Amsterdam, 1978).

[15]David A. Liberman, Phys. Rev. D **16**, 1542 (1977).

[16]V. G. Neudatchin, Yu. F. Smirnov, and R. Tamagaki, Prog. Theor. Phys. **58**, 1072 (1977); Yu. F. Smirnov and Yu. M. Tchuvil'sky, Inst. of Nuclear Physics, Moscow State Univ. report, 1977 (unpublished).

[17]H. Schnitzer, Phys. Rev. Lett. **35**, 1540 (1976).

[18]M. B. Kislinger, Univ. of Chicago Report No. EFI78/15, 1978 (unpublished).

[19]The Pauli principle alone requires a $\Delta\Delta$ component in the configurations (2.7) which separates explicitly into two nucleons. This effect has been studied by Smirnov and Tchuvil'sky, Ref. 16. However, a proper treatment of $\Delta\Delta$ mixing must also take into account mixing with channels which separate explicitly into two $\Delta$'s. The latter effect permits a $\Delta\Delta$ component outside of the repulsive core.